Controlling Vibrational Excitation with Shaped Mid-IR Pulses

David B. Strasfeld, Sang-Hee Shim, and Martin T. Zanni[*]

Department of Chemistry, University of Wisconsin–Madison, Madison, Wisconsin 53706, USA
(Received 16 February 2007; published 18 July 2007)

We report selective population of the excited vibrational levels of the T_{1u} CO-stretching mode in $W(CO)_6$ using phase-tailored, femtosecond mid-IR (5.2 μm, 1923 cm^{-1}) pulses. An evolutionary algorithm was used to optimize specific vibrational populations. Stimulated emission peaks, indicative of population inversion, could be induced. Systematic truncation of each optimized pulse allowed for increased understanding of the excitation mechanism. The pulses and techniques developed herein will have broad applications in controlling ground state chemistry and enhancing vibrational spectroscopies.

Sophisticated control over electric fields has generally led to refined control over quantum processes. Such control first took root in NMR spectroscopy, which utilizes radio frequency pulses with carefully selected frequencies, intensities, phases, and durations to precisely manipulate nuclear spins. At the end of the 20th century, pulse shaping in the visible and near infrared regions of the spectrum extended quantum control capability to electronic processes [1,2]. These phase- and amplitude-tailored pulses have been used to optimize second harmonic generation, control chemical reaction yields, and direct energy distributions in numerous systems. During the past year, our lab has developed the first method for shaping pulses directly in the mid-IR [3,4]. Using this method, we report the first example of phase-tailored, mid-IR pulses preferentially populating vibrational levels in the electronic ground state. We also introduce a new method for ascertaining the excitation mechanism by following population transfer over the course of the pulse. The capacity to selectively populate vibrational levels suggests future use in quantum computing [5], driving chemical processes in the ground state [6], or in multidimensional IR experiments [7].

Numerous pulse shapes have been theoretically proposed to enhance ground state vibrational excitation. These shapes include chirped pulses [5] and sequences of transform-limited pulses that form the basis of adiabatic rapid passage and stimulated Raman adiabatic passage methodologies [8]. Pulses with more sophisticated time and frequency profiles were recently predicted to achieve enhanced vibrational excitation and at least partial quantum selectivity by Meier and Heitz [9] using wave packet propagation simulations at experimentally accessible conditions. In contrast to the large body of theoretical work, the only pulses tested experimentally have been linearly chirped [10,11], as linear chirps are straightforward to achieve with material dispersion or a pair of gratings. In this Letter, we find that advanced control over the time profile of mid-IR pulses gives rise to enhanced vibrational selectivity.

The mid-IR pulses used in this investigation are generated by difference frequency mixing the signal and idler outputs of a barium borate-based optical parametric amplifier in a AgGaS$_2$ crystal. These pulses are 55 fs in duration (268 cm^{-1} bandwidth) and tuned to 5.2 μm, so that the largest portion of the bandwidth is slightly lower in energy than the fundamental antisymmetric transition at 1983 cm^{-1}. A large portion of each pulse is sent through a germanium acousto-optic modulator-based pulse shaper with up to 500 elements of control over phase and intensity [3]. The resulting shaped pulses serve as the pump (1.5 μJ), while the unshaped portion of each pulse serves as the probe ($\sim$50 nJ). At this intensity, the probe pulse operates in the linear regime. Both pump and probe pulses are focused to a 190 μm diameter spot size at the sample, yielding a pump electric field strength of 0.60 GV/m when transform limited. The transient absorption spectra are generated by optically chopping the pump pulse at half of the repetition rate of the laser, so that $\Delta OD = -\ln(\text{transmission}_{\text{pump on}}/\text{transmission}_{\text{pump off}})$ can be computed. Stimulated emission is identified by negative features in the pump-probe spectra as more light hitting the detector leads to an apparent decrease in ΔOD. The phase of the shaped pump pulses was altered using a sum of sine waves that serve as a basis set for the shaper in accordance with the equation:

$$\phi(\omega) = \sum_{i=1}^{4} a_i \sin(b_i \omega + c_i),$$

where ω spans the frequency range of the pump. Using the probe spectrum for feedback, a_i, b_i, and c_i were optimized using an evolutionary algorithm to find the best coefficients for the desired outcome [12]. This basis set was chosen to approximate the pulse shapes that Meier and Heitz predicted would optimize the vibrational excitation of the metal carbonyl in carboxyhemoglobin [9] while simultaneously limiting the dimensions of the control space [13]. We found that four sine waves were the fewest necessary to achieve the desired optimization. Since only phase shaping is used, the pump energy was identical for all of the experiments reported here. The probe spectrum was dispersed through a monochromator and collected on a 32 element mercury cadmium telluride detector. Pulse optimizations were conducted at a pump-probe delay time of 3 ps.

TABLE I.   Relative vibrational populations of $v = 1$–7 for a transform-limited pulse and each optimized pulse from fits of the peak intensities. Improvement factors are calculated relative to a transform-limited pulse.

| Pulse type | Relative vibrational populations | | | | | | | Improvement factor |
	$v = 1$	$v = 2$	$v = 3$	$v = 4$	$v = 5$	$v = 6$	$v = 7$	
Transform-limited	65.8	18.9	8.7	3.9	1.7	0.8	0.3	⋯
$v = 1$–2/0–1 Optimized	88.4	6.6	3.0	1.2	0.4	0.2	0.1	2.2
$v = 2$–3/1–2 Optimized	12.3	58.0	15.5	8.1	3.7	1.7	0.7	4.8
$v = 3$–4/2–3 Optimized	30.7	19.5	29.9	14.5	4.4	0.9	0.2	5.8

Shorter delays were also tried, but we systematically found the optimally shaped pump pulses to have durations in excess of 2 ps. Optimizations required no more than 40 generations for convergence, using the difference in the targeted peak amplitudes as the fitness parameter. Improvement factors were calculated relative to the transform-limited pulse and are reported in Table I. Following each optimization, the best-fit pulse was characterized in the time domain by linear cross correlation with the unshaped probe pulse. $W(CO)_6$ is solvated in *n*-hexane at a concentration that yielded an optical density of 0.8 at 1983 cm^{-1} for a path length of 56 mm.

Shown in Fig. 1(a) is the pump-probe spectrum measured for a transform-limited pump pulse (55 fs duration). The spectrum consists of a negative feature at 1983 cm^{-1} followed by a series of positive and progressively weaker peaks at lower frequencies. This spectrum is typical of femtosecond pump-probe studies. The negative feature corresponds to a bleach of the ground state and $v = 1$–0 stimulated emission. The positive peaks are sequence bands arising from $v = 1$–2, 2–3, 3–4, etc., absorptions, the first three appearing at 1970, 1952, and 1933 cm^{-1}. Peak spacings increase due to the character of the normal mode and match previously reported data [14]. The diminishing peak intensities indicate that a transform-limited pulse becomes increasingly less efficient at populating progressively higher vibrational levels. Shown in Figs. 1(b)–1(d) are the pump-probe spectra resulting from three different pulse optimizations. In Fig. 1(b), the pump pulse has been optimized to maximize the ratio of the intensity of $v = 1$–2 versus $v = 0$–1. Figures 1(c) and 1(d) correspond to optimizing $v = 2$–3 vs 1–2 and $v = 3$–4 vs 2–3, respectively. For comparison, all 4 spectra have been normalized with respect to their ground state bleaches. The normalization constants all lie within a factor of 2, indicating that the absolute excitation efficiency is comparable for the optimized pulses. These optimizations improved the ratio of the targeted peaks by 2.2–5.8 times the transform-limited pulse (Table I). Running Fourier transforms of the three optimized pulses are shown in the top row in Fig. 2 (the convolution width of the Gaussian used in these running Fourier transforms was 215 fs), where $t = 0$ corresponds to the center of the shaped pulse. The optimized pulse shapes grow increasingly more complex for higher vibrational quanta, which we discuss below.

To interpret the pump-probe spectra, one needs to consider that the probe pulse interrogates the vibrational populations through both absorption ($v \rightarrow v + 1$) and stimulated emission ($v + 1 \rightarrow v$). Absorption causes a positive peak in the pump-probe spectrum, whereas stimulated emission peaks are negative. Thus, when $v + 1$ has a larger population than v, a negative peak appears, indicating that the vibrational populations are inverted. Population inversion was achieved in all three cases studied here. Optimizations of the two highest sequence bands exhibited stimulated emission peaks, whereas the signature for population inversion in the fundamental optimization is the larger absolute intensity of the $v = 1$–2 over the $v = 0$–1 transitions, since the ground state cannot cause stimulated emission. To quantitatively extract the relative vibrational populations from the pump-probe spectra, we fit the peak intensities assuming a harmonic scaling law for the transition dipoles [e.g., $(n + 1)|\mu_{n,n+1}|^2 = (n + 2)|\mu_{n+1,n+2}|^2$]
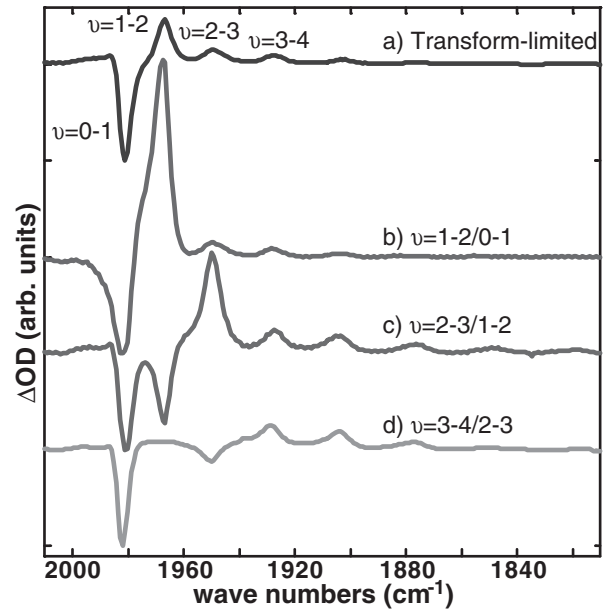

FIG. 1.   Experimental pump-probe spectra for $W(CO)_6$ in *n*-hexane performed with (a) a transform-limited pump pulse, (b) a pulse optimizing the $v = 1 - 2$ vs 0–1 features, (c) a pulse optimizing the $v = 2 - 3$ vs 1–2 features, and (d) a pulse optimizing the $v = 3$–4 vs 2–3 feature.

as has been done previously [14]. The results are given in Table I.

To investigate how these pulses create the populations that they do, we have monitored the evolution of the vibrational populations during the growth of the pump pulses. In principle, the probe can interrogate the sample even during the pump pulse duration, but in practice nonresonant contributions distort the signal. Instead, we used our shaper to systematically truncate the optimized pump pulses in the time domain and then probed the sample 5 ps later, thereby observing how the pump shifts populations during its duration. Such truncation is accomplished by using the optimized mask to generate a time domain profile of the electric field, truncating that time domain profile, and Fourier transforming into the frequency domain to create the required amplitude and phase-tailored mask. The finite bandwidth of the shaped pulse cannot perfectly reproduce a step function, and so a small amount of leakage intensity (<4%) persists for ~3 ps, which is why a 5 ps delay was used. Probing at 5 versus 3 ps negligibly alters the results, since $W(CO)_6$ lifetimes are tens to hundreds of picoseconds (reported below). Shown in Fig. 2 are the intensities of the fundamentals and the first three sequence band peaks as a function of the pulse truncation. Also shown are the corresponding vibrational populations, calculated for each step in the truncation. For the $v = 1$–2 vs 0–1 optimization, the pump consists of 7 pulses separated by ~1 ps [see the running Fourier transform in Fig. 2(a)]. Each of these pulses induces a bleach in the ground state and an increase in the first sequence band, thereby improving the desired outcome in a monotonic fashion. The $v = 2$–3/1–2 and $v = 3$–4/2–3 optimized pumps also consist of pulse trains, although the pulses have alternating intensities and are more closely spaced (~250 fs). For these two optimizations, each pulse in the train improves the ratio by increasing the desired absorption peak intensity at the expense of the fundamental $v = 0$–1 transition, thereby moving the population into the preferred excited vibrational level. However, about midway into the pulse train, the pump begins to depopulate the intermediate vibrational levels in order to transfer the population to the highest level, thereby creating an inverted population. For example, in the $v = 2$–3/1–2 optimization, the $v = 1$–2 peak begins to lose intensity at $t = 0.5$ ps with a resulting decrease in population. A similar process occurs for the $v = 3$–4/2–3 optimization, except that both intermediate levels lose population. It is especially interesting that this population decrease occurs even while the fundamental transition continues to bleach, indicating that the population is still flowing out of $v = 0$.

With these shaped mid-IR pulses now in hand, it is straightforward to measure vibrational population times. Population relaxation is an active research area in condensed phase chemistry because solvent-induced relaxation influences chemical reactivity. Since the carbonyl modes of $W(CO)_6$ have a small anharmonicity and its frequencies are far removed from other modes, the lifetimes might be modeled as a harmonic oscillator linearly coupled to a harmonic bath [15]. If this is true, then they should scale linearly to the vibrational quantum number. Nonlinear trends might be caused by degeneracies with intramolecular sequence and combination bands to give level-specific relaxation rates similar to what is observed in H_2O [16]. Previous publications have extracted the vibrational lifetimes of $W(CO)_6$ using infrared pump-probe spectroscopy with transform-limited pulses [17]. However, extracting the lifetimes is complicated by the fact that transform-limited pulses excite an uncontrolled range of excited vibrational levels as demonstrated in Fig. 1(a). Thus, the decays of all of the peaks must be fit simulta-
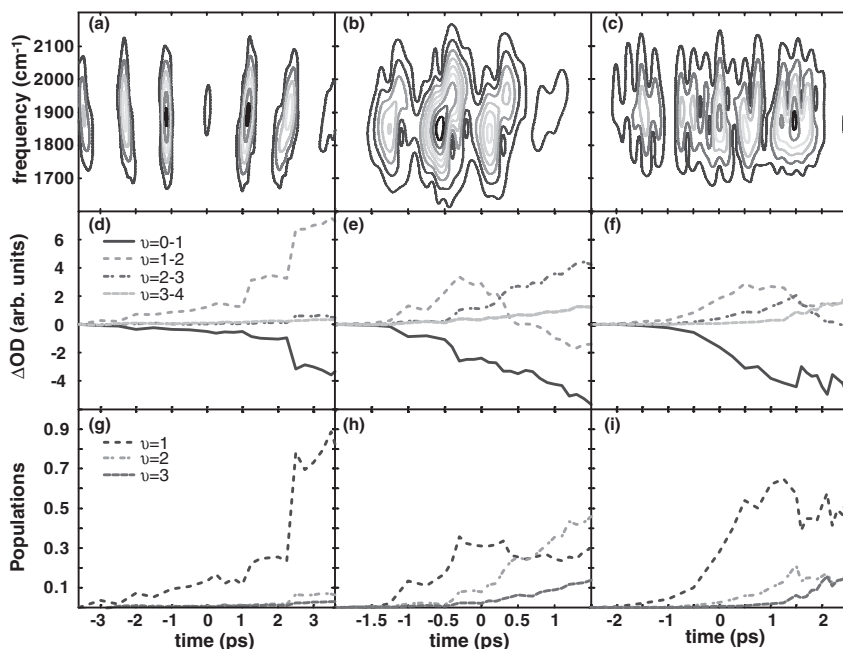
FIG. 2.   (a)–(c) Running Fourier transforms of the linear cross correlations taken for those laser pulses used in Fig. 1 to optimize the $v = 1$–2/0–1, $v = 2$–3/1–2, and $v = 3$–4/2–3 feature ratios, respectively. Contour levels are shown in 10% spacings from minimum to maximum intensity. (d)–(f) Amplitudes of the first four peaks are plotted as a function of the pulse truncation. The fraction of the pulse that was truncated decreases from left to right, so that +3 ps corresponds to the full pump pulse. (g)–(i) Relative populations of the first three vibrational levels extracted from fits.
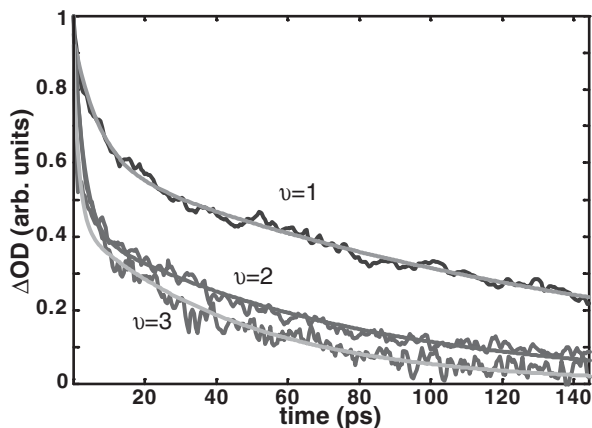
FIG. 3.   Vibrational lifetimes were obtained for the $v = 1$, $v = 2$, and $v = 3$ vibrational levels using pulses optimized to eliminate the population of levels above that which was being measured.

neously to account for population flow from upper levels into lower levels, a calculation whose accuracy is limited by uncertain quantities such as electrical anharmonicity. However, our shaper can suppress higher vibrational population, thereby negating the need for a coupled equation approach. To this end, we optimized a series of pulses that avoided exciting vibrational levels higher than the one desired and then monitored the lifetime with the femtosecond probe as shown in Fig. 3. The relative pump and probe beam polarizations were oriented at the magic angle to eliminate the contribution from orientational motion. We fit only the highest absorption peak to a biexponential decay, which yields a long-time component that corresponds to relaxation of the T_{1u} stretching manifold. The shaped pulses all had durations (~ 4 ps) much less than the relaxation times and were thus neglected in the exponential fits. Previous studies suggest that the fast decay component of the fits corresponds to intermode energy transfer from the infrared-active T_{1u} mode to the Raman active E_g mode [18]. The long-time components of the fits yield population relaxation (T_1) times of $152(\pm 30)$, $75(\pm 20)$, and $46(\pm 15)$ ps for $v = 1$, 2, and 3, respectively. The T_1 times scale approximately with the quantum number, indicating that harmonic solvent/solute coupling models are appropriate to describe the vibrational relaxation for $W(CO)_6$ in *n*-hexane.

In this Letter, we have demonstrated that ground state vibrational populations can be effectively controlled with properly phase-tailored mid-IR pulses. To our knowledge, this is the first example of ladder climbing exhibiting selective ground state control. Furthermore, by systematically truncating the shaped pump pulses, we have studied how the optimized pulses achieve the desired outcome. The excitation mechanism observed here is similar to simulations [9]. More flexible phase- and amplitude-shaping

algorithms might give rise to even better vibrational selectivity as should more intense pulses. Shaped Raman pulses have been used for selective ground state excitation [19,20]; hence, shaped mid-IR pulses offer a complementary approach to selective ground state excitation. Shaped IR pulses may be especially useful in new 2D-IR spectroscopies [7] where uniquely tailored electric fields may become a commonly used tool for enhancing features and improving signal strengths such as is done in NMR spectroscopy.

*Corresponding author.
zanni@chem.wisc.edu
[1] R. J. Gordon and S. A. Rice, Annu. Rev. Phys. Chem. **48**, 601 (1997).
[2] V. V. Lozovoy and M. Dantus, Chem. Phys. Chem. **6**, 1970 (2005).
[3] S. H. Shim, D. B. Strasfeld, E. C. Fulmer, and M. T. Zanni, Opt. Lett. **31**, 838 (2006).
[4] S. H. Shim, D. B. Strasfeld, and M. T. Zanni, Opt. Express **14**, 13 120 (2006).
[5] C. Gollub, B. M. R. Korff, K. L. Kompa, and R. de Vivie-Riedle, Phys. Chem. Chem. Phys. **9**, 369 (2007).
[6] N. Doslic *et al.*, Phys. Chem. Chem. Phys. **1**, 1249 (1999).
[7] S. H. Shim, D. B. Strasfeld, Y. L. Ling, and M. T. Zanni, Proc. Natl. Acad. Sci. U.S.A. (to be published).
[8] N. V. Vitanov, T. Halfmann, B. W. Shore, and K. Bergmann, Annu. Rev. Phys. Chem. **52**, 763 (2001).
[9] C. Meier and M. C. Heitz, J. Chem. Phys. **123**, 044504 (2005).
[10] V. D. Kleiman, S. M. Arrivo, J. S. Melinger, and E. J. Heilweil, Chem. Phys. **233**, 207 (1998).
[11] C. Ventalon *et al.*, Proc. Natl. Acad. Sci. U.S.A. **101**, 13 216 (2004).
[12] R. S. Judson and H. Rabitz, Phys. Rev. Lett. **68**, 1500 (1992).
[13] M. A. Montgomery, R. R. Meglen, and N. H. Damrauer, J. Phys. Chem. A **110**, 6391 (2006).
[14] T. Witte *et al.*, Chem. Phys. Lett. **392**, 156 (2004).
[15] M. E. Coltrin and R. A. Marcus, J. Chem. Phys. **73**, 2179 (1980).
[16] C. P. Lawrence and J. L. Skinner, J. Chem. Phys. **117**, 5827 (2002).
[17] S. M. Arrivo, T. P. Dougherty, W. T. Grubbs, and E. J. Heilweil, Chem. Phys. Lett. **235**, 247 (1995).
[18] A. Tokmakoff, B. Sauter, A. S. Kwok, and M. D. Fayer, Chem. Phys. Lett. **221**, 412 (1994).
[19] A. M. Weiner, D. E. Leaird, G. P. Wiederrecht, and K. A. Nelson, J. Opt. Soc. Am. B **8**, 1264 (1991).
[20] D. Zeidler *et al.*, J. Chem. Phys. **116**, 5231 (2002).